Seismic vulnerability of existing R.C. buildings: A simplified numerical model to analyse the influence of the beam-column joints collapse

Andrea Borghini, Federico Gusella *, Andrea Vignoli

Department of Civil and Environmental Engineering, University of Florence, Italy

ABSTRACT

In order to evaluate seismic vulnerability of existing reinforced concrete buildings, a simplified approach is proposed to take into account the beam-column joints shear collapse. This collapse is described by a link element which is introduced between column and beam. To develop and verify this element, several comparisons have been performed with experimental results of laboratory test and numerical results obtained by a two-dimensional finite element model specifically carried out for this check.

The link element uses a tri-linear moment–rotation law, compatible with standard Italian and European codes, whose features can be estimated by limited structural and geometrical information, which is a typical situation on older existing structures, and by standard code recommendations.

In order to give a preliminary evaluation of the seismic capacity for existing R.C. frames, taking into account the beam-column joints behaviour, this link element has been introduced in a one-dimensional model of bearing structure of the Unit N.1 of the Santa Maria Annunziata Hospital in Florence (Italy) and pushover analyses have been carried out.

© 2016 Elsevier Ltd. All rights reserved.

1. Introduction

Nowadays, the relevance to take into account the effective Reinforced Concrete (R.C.) beam-column joint behaviour in seismic analysis has been fully understood. Regarding new structures, the classical approach proposed in several standard codes is to prevent the shear collapse of the joints by an adequate design. Following this approach in modelling of the response of R.C. structures to earthquake loading, it is assumed that beam-column joints are rigid. In the context of a performance-based seismic design, previous researches indicate the necessity to take into account the inelastic response of the beam-column joints in determining demands relative to the frame components [1–3]. Particular attention is required in case of seismic vulnerability analysis of older existing concrete buildings. For these structures the concrete beam-column connections were only designed for vertical loads, so that it is necessary to verify, in the seismic vulnerability analysis, the joints' conditions. After the classic approach proposed in [4], several laboratory testing of building subassemblages have been performed (for major references [5]). The check of joints can assume more relevance for exterior ones because of

confinement lack as underlined in [6,7], this aspect has been taken into account in Italian standard code [8,9] which explicitly requires to check exterior joints in seismic vulnerability analysis of older existing structures.

In order to describe the behaviour of R.C. beam-column joints several models have been proposed in literature: from implicit models, where the stiffness and strength loss due to joint damage is modelled by modifying beam and column elements using nonlinear springs or plastic-hinges or both at the member ends [10–14], to explicit macroscopic models, that connect beam and column centerline elements to finite-volume joint macroelements which consider several aspects of the inelastic mechanisms governing joint behaviour [15–24].

Starting from an effective case study, in this paper, a non linear link element is proposed to model joint response within the context of a nonlinear frame analysis.

This zero length element is characterised by a tri-linear bending moment rotation law; it is placed at the beam-end section and rigid offsets are included in the beam and column elements to define the joint physical size. Moreover, an elastic–plastic strip model has been used to take into account the nonlinear behaviour of columns and beams.

Further features, of the proposed link element, are the compatibility with the standard codes, a limited number of parameters, assessable by the engineer from in situ investigations and design

* Corresponding author.

E-mail addresses: borghini@dicea.unifi.it (A. Borghini), fede.guse@libero.it (F. Gusella), avignoli@dicea.unifi.it (A. Vignoli).

reports, and the easy implementation in commercial software packages.

This link element has been checked by a specifically developed two-dimensional finite element model and compared with experimental tests.

Adopting this link element in a one-dimensional numerical model of R.C. planar frame, the proposed approach appears appropriate for predicting, by a pushover analysis, the earthquake response of existing structures for a preliminary vulnerability analysis.

2. The case study

The seismic vulnerability of Santa Maria Annunziata Hospital, in Bagno a Ripoli near Florence (I), has been considered. The hospital was designed in 1966 and built in 1968–1972.

The hospital complex is characterised by distinct buildings, in the following analysis the Structural Unit N.1 has been considered (Fig. 1). This Unit has a basement floor, four floors and a walkable roofing; the plan of the structure is shown in Fig. 2.

In the lack of seismic standard code, the bearing structure was realised by R.C. frames taking into account only vertical loads; the scheme of the central frame, which has been the object of the vulnerability analysis, is shown in Fig. 3.

The analysis of the design documentation and experimental tests permitted to found the geometrical characteristics and reinforcement bars of columns and beams (Fig. 4). Regarding the mechanical characteristics of material, experimental tests permitted to check the data reported in design documentations, in particular the concrete compressive strength was f_{cm} = 22.5 N/mm^2 while the yield strength of high-bond reinforcing bars was f_{ym} = 440 N/mm^2.

3. Two-dimensional numerical model and comparison with experimental results

The first part of the study has been devoted to tune-up a finite element numerical model capable to describe the nonlinear behaviour of the beam-column joints and underline the main parameters that influence their behaviour; this model has been developed adopting DIANA-TNO code [25]. The model has been realised by two-dimensional mesh with eight nodes isoparametric elements in plane stress. Regarding the concrete behaviour, the smeared cracking model for tension and elastic–plastic stress–strain law for compression have been used. The Drucker–Prager criterion was adopted in compression taking into account the increasing of strength capacity in bi-axial compression. Following [26], the maximum compressive strength increases approximately 16% under conditions of equal biaxial compression $\sigma_1/\sigma_2 = 1$ and about 25% increase is achieved at a stress ratio of $\sigma_1/\sigma_2 = \sigma_2/\sigma_1 = 0.5$; to obtained these conditions, the parameters of the Drucker–Prager failure surface were: friction angle $\varphi \approx 10°$ and cohesion c = 42% of the compression strength; moreover to ensure an associated plasticity the dilatation angle has been chosen equal to friction angle [25].

The Rankine criterion has been adopted to bound the tensile strength; moreover the linear stress cut-off criterion was considered: the fracture is activated when the traction overcomes the values f_t or $f_t (1 + \sigma_{lateral}/f_{cm})$ where $\sigma_{lateral}$ is the lateral stress and f_t is the traction strength. In this way an overall Rankine/Drucker–Prager criterion has been obtained to model the strength of concrete.

Relative to smeared formulation of cracks in concrete, once the concrete reaches its tensile strength it exhibits a tensile softening response. The post-peak tensile stress–strain relationship has been

Fig. 1. Unit N.1 of the Santa Maria Annunziata Hospital, Bagno a Ripoli, Florence (I).

approximated by the cubic exponential curve proposed by Hordijk [27,28], where the ultimate crack deformation was obtained adopting the Mode-I fracture energy G_f proposed in Model Code 90 [29] and the crack bandwith as proposed in [25]. The steel reinforcements have been modelled by "bar embedded reinforcements" [25].

Before using the previously described numerical model to analyse the R.C. frame joints of the case study (Unit N.1), the model has been checked by comparison with experimental results. Several experimental research programs have been performed in the recent years; references are reported in [1,5,20]. Taking into account the successive application of the numerical model to the Unit N.1, the experimental results of the research activity in the framework of DPC-RELUIS – project (research line 2) [30,31] have been considered for similarity to the case study in terms of material characteristics and mode of construction. The structural scheme used in the experimental test and numerical simulations is shown in Fig. 5(a).

During those experimental programs, quasi-static cyclic tests have been carried out on full scale exterior beam-column joints, designed with different earthquake resistant level, axial force value and type of steel reinforcement. The main characteristics, in terms of geometric details and steel reinforcements, of the considered specimens T1, T6, T5 and T3 are summarised in Table 1. In particular NE corresponds to the specimens that were designed taking into account the vertical load, while the seismic load was considered for specimens Z2. The mechanical characteristics of materials were: R.C. compressive strength f_{cm} = 21.5 N/mm^2, yield strength of steel bars f_{ym} = 478 N/mm^2.

The experimental set-up had the following restraints (Fig. 5(a)): a simple support at the section (Q) of the beam and a hinge at the bottom section (R) of the column. The vertical load N and the horizontal load T were applied to the free upper section (P) of the column. As reported in Table 2, NL corresponds to a limited value of the axial force, NH corresponds to a greater value, in particular $v = N/(bhf_{cm})$ is the dimensionless force, with b and h geometric dimensions of the column cross-section.

The tests were characterised by different collapse: B corresponds to flexural collapse of the beam and B + J correspond to beam-joint collapse where T_u is the maximum load and D_u is the drift with a 20% reduction of the maximum load, Table 2.

The experimental tests were simulated by the previously described numerical model and the obtained results were in adequate accord with the experimental ones both for beam collapse and beam-column joint collapse. As shown in Table 2, the differences between numerical and experimental tests, in terms of maximum horizontal force T_u and dissipated energy E, are limited. Moreover the numerical model appears describe properly the collapse behaviour and take into account the effect of the axial force in the column, in fact a smaller value of vertical load
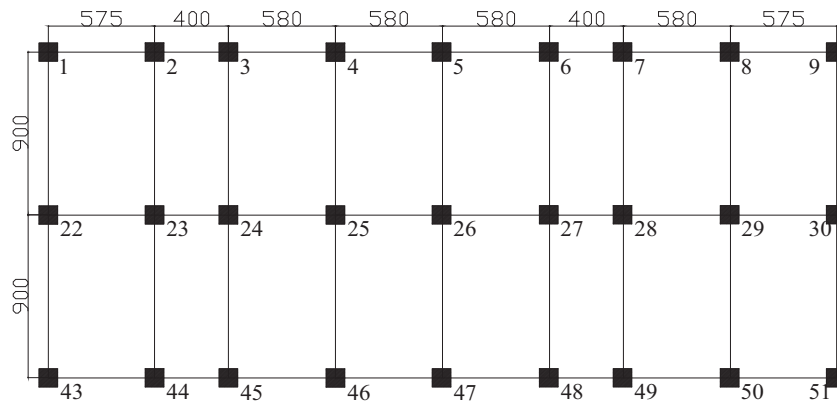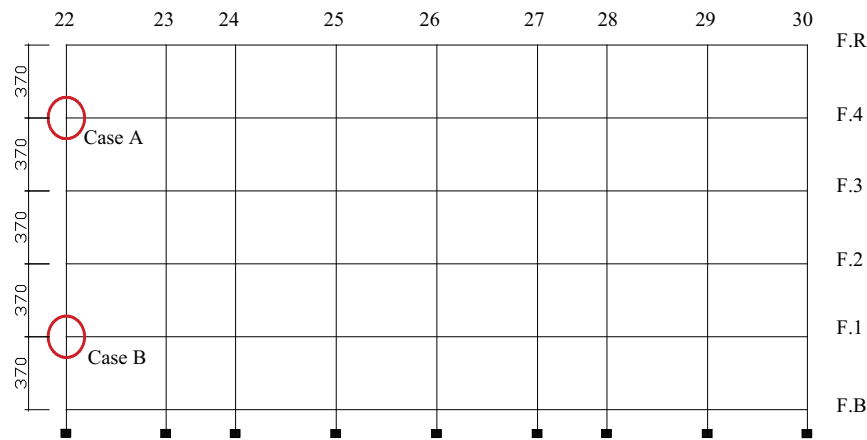
Fig. 2. Plan of the Unit N.1 (cm).

Fig. 3. Scheme of the central frame and beam-column joints analysed by numerical model (case A and case B) (cm).

(see comparison between *T5* and *T3*) facilitates the damage in the joint due to smaller confinement effect.

It should be noted that the maximum horizontal force T_u is grater in T5 specimen (*collapse type B + J*), designed for seismic action, respect to T1 (*collapse type B*), designed only for vertical loads and characterised by the same axial force *N* applied on the column; at the same time, the joint shear demand in T5 is greater than in T1 because of the greater bending moment in the beam; this gives rise to a brittle collapse of the beam-column joint.

A consequence of the beam-column joint collapse is a lesser drift D_u respect to that of T3 specimen (*collapse type B*) whose mechanical features are equal to T5 specimen but characterised by a greater value of axial force *N* in the column; more details about numerical check are reported in [32].

4. Analysis of the joints of the case study

From the effective design report, the design charts (Fig. 4) and the results of an identification-survey program, two types of beam-column joint have been selected ("case A" and "case B" Fig. 3), these joints are both external because they, due to the confinement lack, are more prone to collapse during the seismic events [6–9].

The characteristics of the beam 22–23 (Fig. 3) were equal for all floors and are reported in Table 3. Using a classic approach the maxima of bending moments have been calculated and reported in Table 3 too. The characteristic of columns are reported in Table 4; the axial forces have been calculated using the values of vertical loads reported in the standard code NTC 2008 [8].

Considering the structural scheme reported in Fig. 5(a) (equal to the one utilised in experimental test previously cited), a first analysis has been performed using a finite element program [33] with one-dimensional elements where the nonlinear behaviour is taken into account by an elastic–plastic strip model. Regarding the material behaviour the Mander's model [34] and bilinear model were used for concrete and steel bars, respectively. In this analysis the beam-column joint has been assumed infinitely rigid with an infinite strength.

The analysis was conducted increasing the horizontal displacement of the top of the column (section (P)). For both structural cases (case A and case B) the collapse was reached in the beam near the column (*collapse type B*) with a value M_{rd}^+ that was in accordance with analytical evaluation (Table 3). The equilibrium condition permits to evaluate the vertical force of the restraint Q

$$V_{max} = M_{rd}^+/L^* \tag{1}$$

with $L^* = L - h/2$ where *h* is the height of column cross section; the maximum horizontal force at the top of the column, that produces the displacement at the collapse, is

$$T_{max} = V_{max} \cdot L/H \tag{2}$$

Given that the beams were equal in A and B cases, the maximum horizontal force was equal ($T_{max} \approx 67$ kN, see Table 5); it should be noted that in this numerical approach the axial force in the column does not have effects.
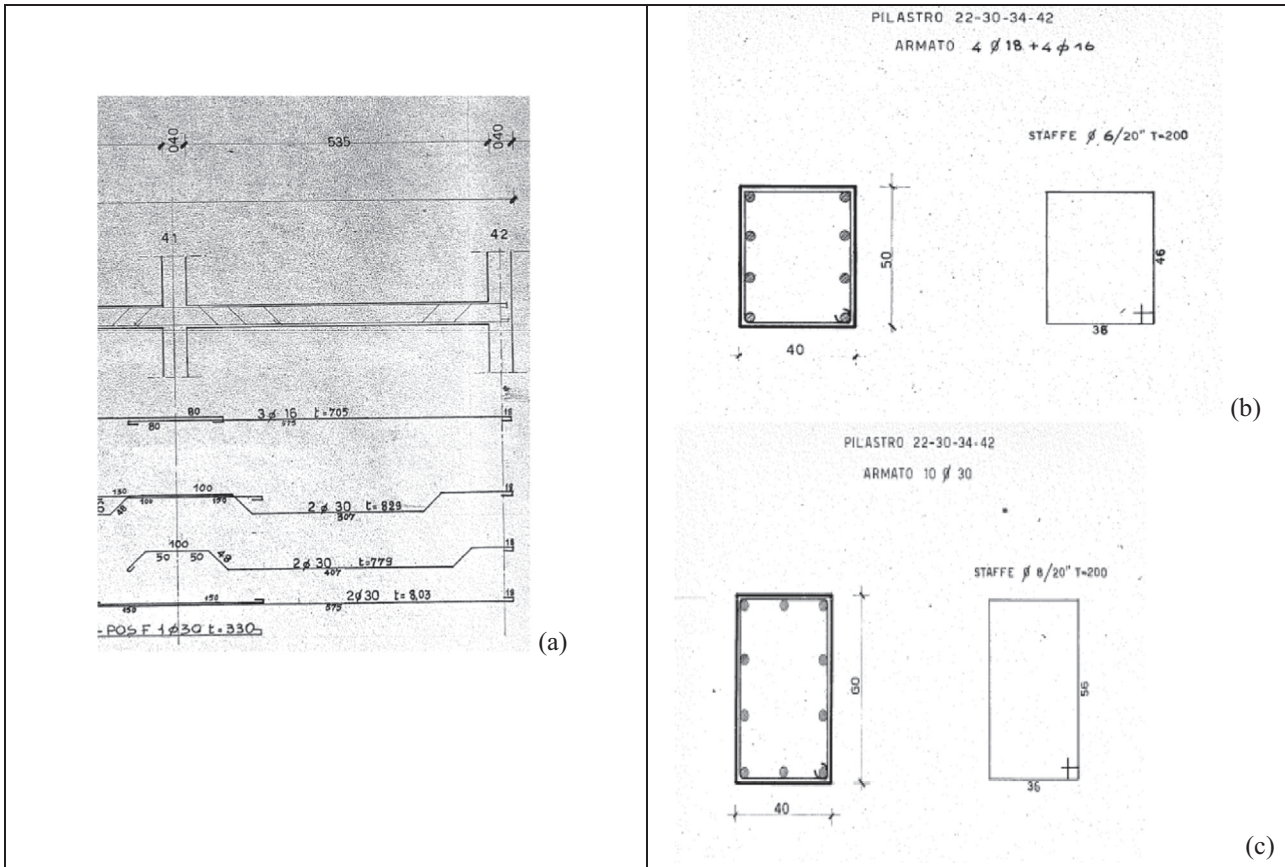
Fig. 4. Design charts: (a) characteristics of the external beam (this beam was equal to the beam 22–23 analysed by two-dimensional finite element model); (b) characteristics of the column from floor 2 to floor R; (c) characteristics of the column from floor B to floor 2.
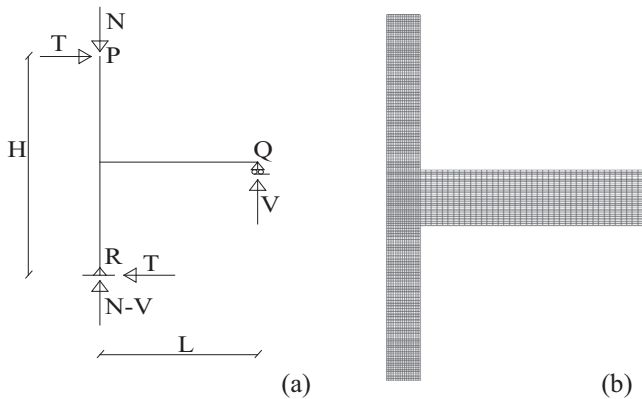

Fig. 5. (a) Structural scheme used for the analysis of R.C. beam-column joints, (b) finite element mesh.

In order to highlight the effect of the beam-column joint damage, the cases A and B have been also analysed using the previously described two-dimensional numerical model; the mesh is shown in Fig. 5(b). This approach can be acceptable because of the good similarity, in terms of material mechanical characteristics (values of the concrete compressive strength and yield strength of high-bond reinforcing bars) and dimensionless structural parameters, between experimental tests [30], previously used to check the two-dimensional model, and the joints of case study.

In particular, the values of the parameter $v = N/(bhf_{cm})$ (typical of older existing R.C. structures that were built using the allowable stress design with only vertical loads, see Tables 2 and 4) are similar, except for the joints on the top of the frame; nevertheless these joints, as shown in the following, have a joint shear collapse so that a lesser value of v does not modify the expected brittle behaviour of the joints and the two-dimensional model results are in the safe side.

Table 1
Geometric details and steel reinforcements of the experimental joints of DPC-RELUIS – project [30,31].

Characteristics of tests			Beam						Column				
Specimen	Design	Axial force (kN)	b (m)	h (m)	L (m)	Af'	Af	As	b (m)	h (m)	H (m)	$Af = Af'$	As
T1	NE	290	0.3	0.5	2	2Ø12	2Ø12	1Ø8/25 cm	0.3	0.3	3.2	2Ø14	1Ø8/20 cm
T6	NE	580	0.3	0.5	2	2Ø12	2Ø12	1Ø8/25 cm	0.3	0.3	3.2	2Ø14	1Ø8/20 cm
T5	Z2	290	0.3	0.5	2	3Ø16	2Ø16 + 1Ø12	1Ø8/25 cm 1Ø8/10 cm*	0.3	0.3	3.2	3Ø14	1Ø8/20 cm 1Ø8/7.5 cm*
T3	Z2	580	0.3	0.5	2	3Ø16	2Ø16 + 1Ø12	1Ø8/25 cm 1Ø8/10 cm*	0.3	0.3	3.2	3Ø14	1Ø8/20 cm 1Ø8/7.5 cm*

b, h base and height of the cross section; L, H length of the beam and column (Fig. 5a); Af' upper reinforcement; Af bottom reinforcement; As shear reinforcement, * around joint.

Table 2
Characteristics and results of the experimental tests in the framework of DPC-RELUIS – project [30,31], comparison with numerical results obtained by two-dimensional model in terms of percentage difference between maximum horizontal force (ΔT_u) and dissipated energy (ΔE).

Characteristics of tests				Experimental results			Numerical results			Differences	
Specimen	Design	Axial force	$v = N/(bhf_{cm})$	Collapse type	$D_u = d/H$ (%)	T_u (kN)	Collapse type	$D_u = d/H$ (%)	T_u (kN)	ΔT_u (%)	ΔE (%)
T1	NE	NL	0.15	B	2.75	19	B	2.75	21	11	14
T6	NE	NH	0.30	B	2.85	21	B	2.85	20	−6	−3
T5	Z2	NL	0.15	B + J	3.25	40	B + J	1.7	46	15	−19
T3	Z2	NH	0.30	B	4.96	39	B	4.96	46	19	18

Table 3
Geometric details and steel reinforcements of beam 23–22; Af' upper reinforcement; Af bottom reinforcement; As shear reinforcement; M_{rd}^+ and M_{rd}^- design values for bending moment; A, b, h area, base and height of the beam cross-section.

Beam							
Af'	Af	As	M_{rd}^+ (kN m)	M_{rd}^- (kN m)	b (m)	h (m)	A (m^2)
3Ø16 + 4Ø30	2Ø30	1Ø10/25 cm	230	545	1.2	0.4	0.48

Table 4
Geometric details and steel reinforcements of external columns (Fig. 3, No. 22); b, h base and height of the cross-section; A cross section area; Af reinforcement; As shear reinforcement; N axial force; M_{rd} design values for bending moment.

Column	b (m)	h (m)	A (m^2)	$Af = Af'$	As	N (N)	M_{rd} (kN m)	$v = N/(bhf_{cm})$
F.B-F-1	0.60	0.40	0.24	4Ø30	1Ø8/20 cm	892	590	0.17
F.1-F.2	0.60	0.40	0.24	4Ø30	1Ø8/20 cm	753	573	0.14
F.2-F.3	0.50	0.40	0.20	2Ø18 + 2Ø16	1Ø6/20 cm	560	242	0.12
F.3-F.4	0.50	0.40	0.20	2Ø18 + 2Ø16	1Ø6/20 cm	371	212	0.08
F.4-F.R	0.50	0.40	0.20	2Ø18 + 2Ø16	1Ø6/20 cm	184	180	0.04

Table 5
Comparison of numerical results.

Characteristics of specimens		One-dimensional model (rigid joint)		Two-dimensional model	
Case	Axial force (kN)	Collapse type	T_{max} (kN)	Collapse type	T_{max} (kN)
A	184	B	67	B + J	60
B	753	B	67	B	67

Further experimental tests and comparisons should be carried out for higher values of $v > 0.3$.

In the case A, the numerical analysis showed an early collapse of the beam-column joint (*collapse B + J*) with a reduction of the maximum horizontal force $T_{max} \approx 60$ kN (Table 5). In the case B, the axial force, higher than in case A, gives a confinement effect for the concrete in the joint and permits to have the collapse of the beam (*collapse B*) reaching an horizontal force similar to that obtained by the one-dimensional model with rigid joint, $T_{max} \approx 67$ kN (Table 5). Regarding the stiffness of the structural numerical models (Fig. 6), it is equal in the beginning elastic field; after it is possible to observe a deterioration in the one-dimensional model, when cracking bending moment is achieved in the end section of the beam, greater than two-dimensional model characterised by a smeared cracking approach.

A third model (case C) was considered where the two-dimensional mesh elements of the joint were assumed infinitely elastic; the comparison is shown in Fig. 7, where it is possible to observe a grater stiffness of the structural case that does not take into consideration the mechanical degradation of the beam-column joint; in this case the maximum horizontal force, similar to case B and that determines the maximum bending moment in the beam, is reached.

Considering the stress field in the joint, the case A is characterised by the presence of a narrow strut (Fig. 8(a)) where the averaged compression in the concrete achieves a high value (green colour[1] in Fig. 8(a)), about its maximum value $f \approx 1.16 f_{cm} \approx 26$ MPa in accordance with the Kupfer and Gerstle model [26]. In the case B (Fig. 8(b)), the strut width is greater so that the averaged compression is lesser than in case A ($f \approx 18$ MPa) (light orange colour in Fig. 8(b)).

The crack pattern is shown by blue and green lines in Fig. 9; from numerical results, in the case A the cracks are greater than those of the case B and affect mainly the joint panel. Moreover the larger cracks of the case B (green colour in Fig. 9(b)) are located in the bottom of the beam, so the brittle collapse of the joint is postponed.

The early damage in the joint (case A) does not permit to reach the plastic bending moment in the beam section (case B), this can also be explained considering the interaction between the stresses in the concrete and in the reinforcement bars.

In fact for the case C, where the joint has been modelled by elastic finite elements, the plastic bending moment of the beam is achieved at the section XX (Fig. 10(a)), with ultimate stresses for the concrete (maximum compression in the top of the beam $f = f_{cm} = 22.5$ N/mm^2, dark green colour in Fig. 10(a)), and the reinforcement bars (maximum traction in the bottom of the beam $f = f_{ym} = 440$ N/mm^2, red colour in Fig. 10(b)).

Furthermore the stress in the beam reinforcement bars, for increasing column top displacements, are shown in Fig. 11; the numerical analysis showed that the stress was lesser when the joint's damage was greater and only in the case B, characterised by the collapse of the beam (*collapse B*), the traction stress achieved its maximum value.

---

[1] For interpretation of color in Figs. 8–10, the reader is referred to the web version of this article.
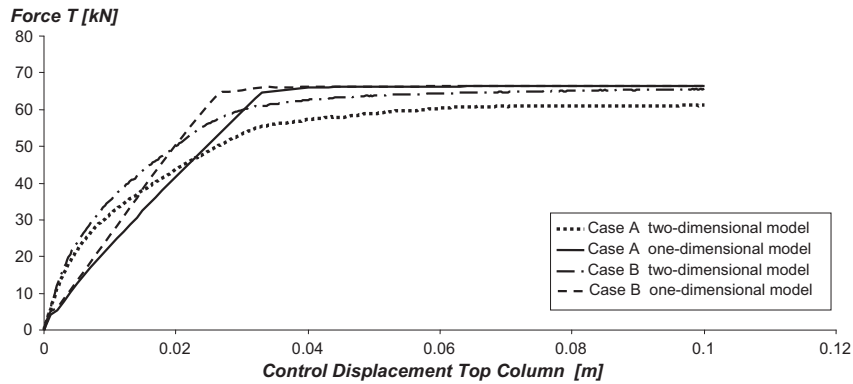
Fig. 6. Capacity curve for case A and case B, comparison between one-dimensional and two-dimensional numerical model.
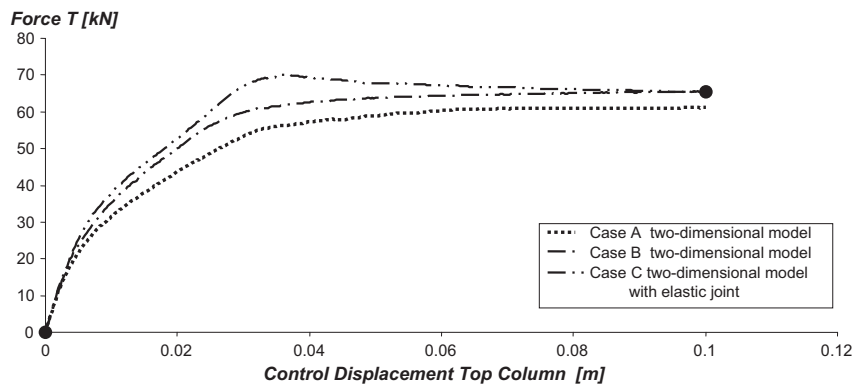

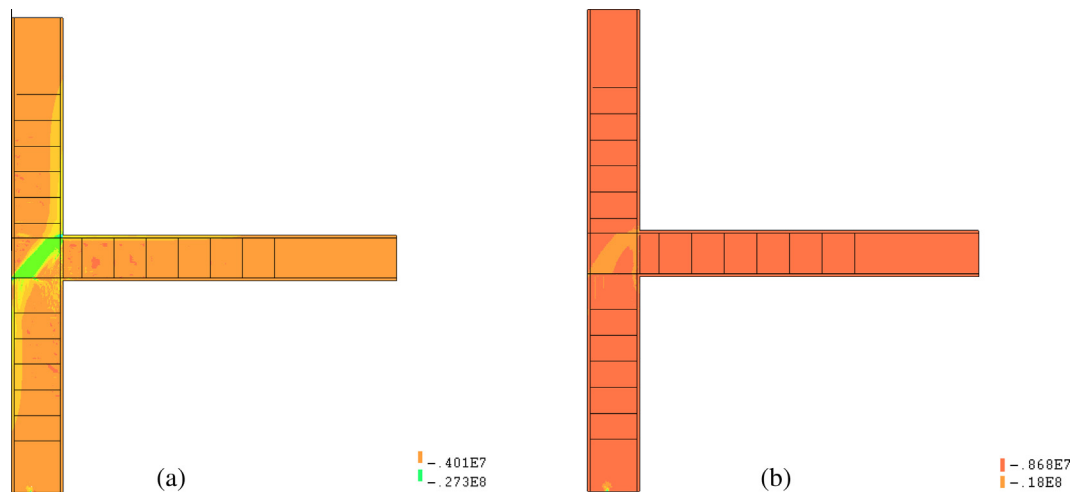**Fig. 7.** Capacity curve, comparison among case A, case B and case C (infinitely elastic joint).

Fig. 8. Compression stress (N/m²), (a) for the case A, (b) for the case B (results for column top displacement ≈ 10 cm).

An additional effect of the joint collapse is the reduction of the structural ductility as highlighted in several experimental tests [30,31]. The numerical results relative to case A confirm this reduction, in fact the numerical convergence was reached only for a displacement smaller than in case B (or C). This reduction can be described by an ultimate rotation of the plastic hinge, at the beam end section, smaller than that relative to case without brittle collapse of the joint. In the performed analyses, the numerical results showed this reduction about 30%; this value appears in sufficiently accordance to observations reported in literature [5].

In conclusion the numerical analyses confirmed that beam-column joint collapse can influence the elasto-plastic behaviour, in terms of maximum shear and ductility, and that a classic one-dimensional numerical model, only capable to describe plasticity of the beam, cannot give reliable results. On the other hand it is necessary to use one-dimensional models to conduct global analysis of large structure as reinforcement concrete frames. In order to obtain a one-dimensional numerical model capable to take into account the effective joint panels behaviour and give a sufficiently adequate response, a link element has been introduced between
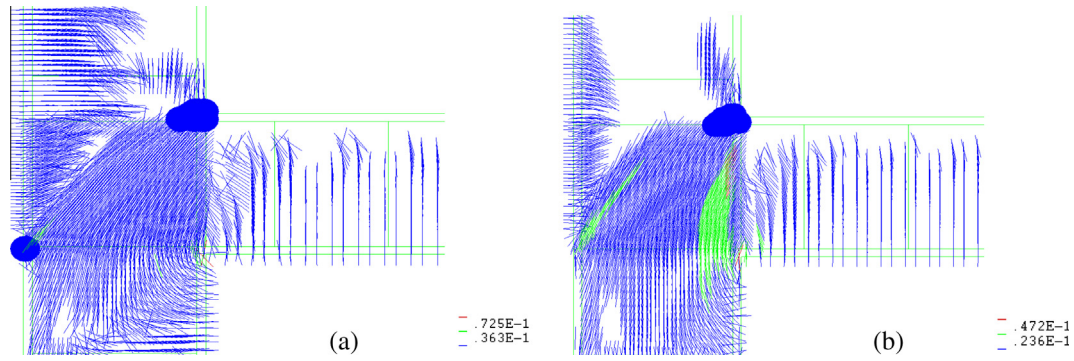
Fig. 9. Cracks in the beam-column joint, (a) for the case A, (b) for the case B (results for column top displacement ≈ 10 cm).
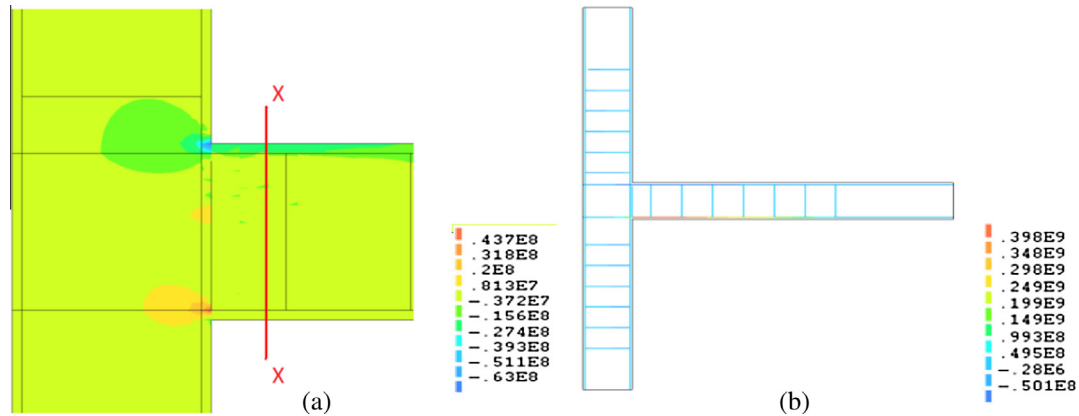

Fig. 10. (a) Stress in concrete and (b) stress in reinforcement bar (N/m²) for case C with elastic joint (results for column top displacement ≈ 10 cm).
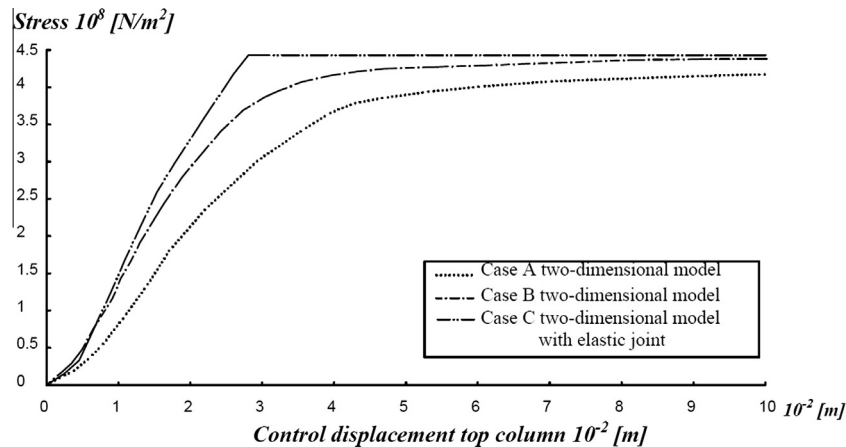

Fig. 11. Traction stress (N/m²) in beam reinforcement bars (section X–X, Fig. 10) for case A, case B and case C.

beam and column; the procedure to define the characteristic of this link and the application to the frame of the Unit N.1 are reported in the following.

5. Ultimate shear force evaluation

Nowadays several standard codes consider the design of the beam-column joint and introduce check procedures. In the present analysis the Italian codes [8,9] have been taken into account.

Regarding existing structures, the check is limited to exterior joints and traction stress and compression stress have to respect the following conditions

$$\sigma_{nt} = \left| \frac{N}{2A_g} - \sqrt{\left(\frac{N}{2A_g}\right)^2 + \left(\frac{V_n}{A_g}\right)^2} \right| \leqslant 0,3\sqrt{f_c} \quad (f_c \text{ in MPa}) \qquad (3)$$

$$\sigma_{nc} = \frac{N}{2A_g} + \sqrt{\left(\frac{N}{2A_g}\right)^2 + \left(\frac{V_n}{A_g}\right)^2} \leqslant 0,5f_c \quad (f_c \text{ in MPa}) \qquad (4)$$

where N is the axial force acting on the upper column, A_g is the gross area of the joint panel horizontal section, V_n is the horizontal shear acting in the joint panel, evaluated accounting both the column shear and the shear transmitted by the beam reinforcing bars, and f_c is the concrete strength. Given N and f_c, from previous equations

Table 6
Estimation of the ultimate V_n in the R.C. beam-column joints: $V_{n,1}$ obtained by standard code [minimum value between Eqs. (3) and (4)], $V_{n,2}$ obtained by two-dimensional numerical model $V_{n,2} = M_{max}/z - V_c$ (5).

Case	$V_{n,1}$ (kN)	$V_{n,2}$ (kN)
A	365	543
B	543	625

it is possible to evaluate the ultimate shear force V_n (V_n is the smaller value between (3) and (4)).

Regarding the previously described numerical analyses the ultimate joint shear can be obtained by [4]

$$V_n = M_{max}/z - V_c \qquad (5)$$

where M_{max} is the bending moment of the beam, z is the length of the internal lever arm and V_c in the shear in the column.

By comparison with numerical results it should be noted (Table 6) that the ultimate shear force obtained by (3) and (4) is on the safe side. This was confirmed also considering the experimental tests relative to DPC-RELUIS – project [32].

From previous observation the minimum value V_n, obtained by inversion of (3) and (4), can be used, on the safe side, as maximum shear in the column-beam joint.

6. Preliminary pushover analysis

At first, a pushover analysis of whole frame of the Unit N.1 with rigid joints has been performed using a finite element code [33] with one-dimensional elements; in this case the nonlinear behaviour has been taken into account by an elastic–plastic strip model. Using the internal forces (M_{max}, V_c) obtained in this analysis, the shear forces V_n in the column-beam joints have been calculated by (5).

By these shears and the axial forces N in the columns obtained by the pushover analysis, σ_{nt} (3) and σ_{nc} (4) were calculated and compared with the limit values which have been evaluated in two cases: considering the effective compressive strength f_{cm} or the reduced limit value f_c as proposed by standard code [8,9] for existing R.C. structures; in particular $f_c = f_{cm}/(\gamma_C FC)$ where $FC = 1.2$ and $\gamma_C = 1.5$ are the confidence factor and the partial factor, respectively.

In both cases, it should be noted that every joints do not satisfy the check (Table 7) so that the classical pushover analysis, where beam-column joints were assumed infinitely rigid with an infinite strength, is not reliable. So it is necessary to introduce a "numerical element" in the one-dimensional analysis to take into account the effect of the joint's damage.

In order to realise this numerical element, some preliminary considerations about the influence of the axial and shear force in the column have been taken into account.

The checks (3) and (4) have also been conducted utilising the N axial forces in the columns determined by only vertical loads; the results $\sigma_{nc,v}$ and $\sigma_{nt,v}$ are reported in Table 7, it should be noted that the effect of the column axial force variation, due to seismic action, is limited in the joint check as highlighted by the percentage difference.

Moreover the column shear V_c gives a limited contribution on joint ultimate shear force as reported in Table 8.

Both previously observations will be considered in the following fulfilment of the numerical element describing the beam-column joint.

Table 7
Check of the joints. Results of pushover analysis with rigid joints: diagonal compression σ_{nc} (3), tensile stress σ_{nt} (4); $\sigma_{nc,v}$ and $\sigma_{nt,v}$ obtained with N determined by only vertical loads. Limit values: $0.5f_{cm}$ or $0.5f_c$ for Eq. (3) and $0.3\sqrt{(f_{cm})}$ or $0.3\sqrt{f_c}$ for Eq. (4).

Level store	σ_{nc}	σ_{nt}	$\sigma_{nc,v}$	$\sigma_{nt,v}$	$\frac{(\sigma_{nc}-\sigma_{nc,v})}{\sigma_{nc,v}}$	$\frac{(\sigma_{nt}-\sigma_{nt,v})}{\sigma_{nt,v}}$
4	4.60	3.70	4.57	3.67	0.6%	0.6%
3	7.06	5.14	6.82	4.97	3.4%	3.3%
2	9.13	6.11	8.55	5.74	6.8%	6.3%
1	9.43	5.98	8.60	5.50	9.6%	8.8%
Limit values						
$0.5f_{cm}$ = 11.25		$0.3\sqrt{(f_{cm})}$ = 1.42		$0.5f_c$ = 6.25		$0.3\sqrt{f_c}$ = 1.06

Table 8
Column shear V_c from pushover analysis, V_n joint shear (Eq. (5)).

Floor	4	3	2	1
V_c (KN)	83	108	148	163
V_n (KN)	816	1158	1397	1652
V_c/V_n (%)	10	9.3	10.6	9.9

7. Link element

In the literature several models, with increasing difficulties to represent the effective joint behaviour, are reported.

The implicit models usually introduce springs at the intersection of the beam and column line elements, where the load deformation response of the spring is defined on the base of the shear-stress response of the joint.

For example, El-Metwally and Chen [10] developed a model with a zero length rotational spring at the beam-column intersection, Alath and Kunnath [11] used rigid link with a rotational spring connected to its end, Uma and Prasad [12] modelled the joint region using a flexural rigid shear beam element placed in series with traditional beam/column flexural elements. A two spring joint element was proposed by Biddah and Ghobarah [15] while a dual-hinge lumped-plasticity beam element, which comprises two rotational springs in series, was used by Birely et al. [5].

The advantage of this type of model is its simplicity while the primary disadvantage is the calibration to provide an accurate simulation of joint response. Other disadvantage is the need to define duplicate nodes at the centre of the joint and this is not supported by commercial software.

The second approach for modelling joint behaviour is the explicit macroscopic joint model that connects beam and column centerline elements. Altoontash and Deierlein [21], Lowes and Altoontash [22], and Mitra and Lowes [23] have proposed models that comprise a shear-panel component and rotational springs or zero-length springs. Other macro-models have been developed by several researchers [16–19]. These models, with an adequate calibration, offer the greatest potential for accurately simulating the nonlinear response of joints. The drawbacks of this modelling approach, however, are the large data set required for calibration and that these models are not easily implemented in commercial software.

The aim of the present study was to realise a simplified link element to describe the beam-column joint behaviour. The main requirement is that a structural model with links of a R.C. frame should allow an adequate evaluation of the effect of brittle collapse of joints in a pushover analysis within of the seismic vulnerability estimation.

Differently from approaches proposed in [15], with two springs, and in [11], with one spring and rigid link elements in the node, in the present study, the proposed zero length link element, like in [10], has a nonlinear behaviour and is placed at the beam-end section; moreover rigid offsets, equal to the joint dimensions, have
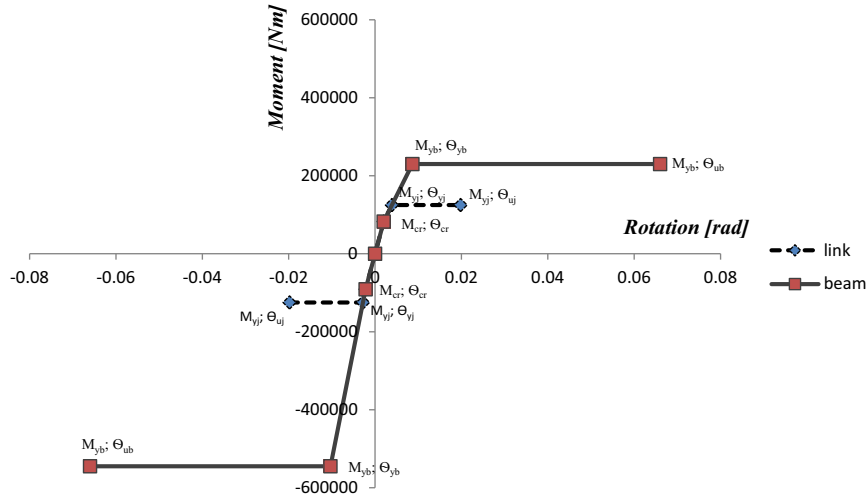
Fig. 12. M–Θ law for link element – case A (bending moment (Nm) – rotation (rad)).

Table 9
T5 specimen: comparison among one-dimensional model, with and without link, and experimental test; case A: comparison among one-dimensional model, with and without link, and two-dimensional numerical model; T_u maximum horizontal load; d_u last displacement; ΔT_u percentage difference between maximum horizontal force; Δd_u percentage difference between maximum displacement.

T5 specimen	Collapse type	$D_u = d_u/H$ (%)	T_u (kN)	ΔT_u (%)	Δd_u (%)
Experimental test	$B + J$	3.2	40		
One-dimensional model with rigid joint	B	5.0	37	8	58
One-dimensional model with link	$B + J$	3.1	37	8	2
Case A	Collapse type	$d_u = d/H$ (%)	T_u (kN)	ΔT_u (%)	Δd_u (%)
Two-dimensional model	$B + J$	3.0	60		
One-dimensional model with rigid joint	B	6.5	67	12	118
One-dimensional model with link	$B + J$	2.9	59	2	3

been included at the ends of the beam and column elements to define the joint volume, following the procedure proposed in [5].

The simplified link element, like [5], has to be appropriate for predicting the earthquake response of planar frames, for which the nonlinearity is controlled by yielding of beams and/or non-ductile response of joints. The link element has been introduced in a one-dimensional model where the nonlinear behaviour of the members (columns and beams) is taken into account by an elastic–plastic strip model, differently from [5] where they were modelled by elastic element and lumped-plasticity beam element respectively.

As suggested in [5], a feature of the proposed link element is to be compatible with the standard code (European and Italian code in the present study), moreover it has to be easily implemented in commercial software packages commonly used for static nonlinear seismic vulnerability analysis; it is noted that further investigations should be required for an adequate application of the proposed link in a dynamic analysis taking into account the degradation of joint cyclic behaviour as proposed in [14].

The proposed link will be defined by a limited number of parameters that can be easy evaluated by the engineer from in situ investigations, design reports or analytical considerations and standard codes. Eventually the link will take into account the observations relative to the influence of axial and shear force in the column, reported in the previous chapter.

Likewise of the approach proposed in [5], the link has been characterised by a moment–rotation law M–Θ; in fact the link has to reproduce the behaviour of the beam when the joint is rigid; this behaviour, in terms of yielding bending moment and ultimate rotation, have to be modified when the joint reaches its maximum shear strength.

In the present study, the link behaviour has been assumed to be described by a tri-linear law M–Θ. At first, the plastic condition of

the beam has been evaluated. This corresponds to classic concrete beam plastic moment M_y and the corresponding capacity which is given by the chord rotation at yielding θ_y [8,9,35]:

$$\theta_y = \phi_y \frac{L_v}{3} + 0.0013\left(1 + 1.5\frac{h}{L_v}\right) + 0.13\phi_y \frac{d_b f_y}{\sqrt{f_c}} \qquad (6)$$

where ϕ_y is the yield curvature of the end section, h is the height of the section, d_b is the (mean) diameter of the tension reinforcement f_c and f_y are concrete compression strength and tensile steel strength, L_v is the ratio moment/shear at the end section.

The yield curvature has been assumed equal to

$$\phi_y = (\varepsilon_c + \varepsilon_{st})/z \qquad (7)$$

where ε_c is the concrete strain and ε_{st} is the steel strain, corresponding to the moment M_y, and z the length of the internal lever arm.

Before reaching the yielding condition, a preliminary change in the law M–Θ is due to the cracking.

The cracking bending moment M_{cr} has been evaluated by the classical approach and in particular the Euler–Bernoulli hypotheses (plane sections remain plane and normal to the axis of the beam) and perfect bond among steel bars and concrete

$$M_{cr} = \frac{\sigma_t J}{(h - x_G)} \qquad (8)$$

with $\sigma_t = f_{ctm}/1.2$ (f_{ctm} traction mean strength), J the second moment of area of concrete section and x_G the centre of the area without cracks.

The chord rotation at cracking θ_{cr} is obtained by Eq. (6) substituting to the yield curvature the cracking curvature

$$\phi_{fess} = \frac{\varepsilon_t}{(h - x_G)} \qquad (9)$$
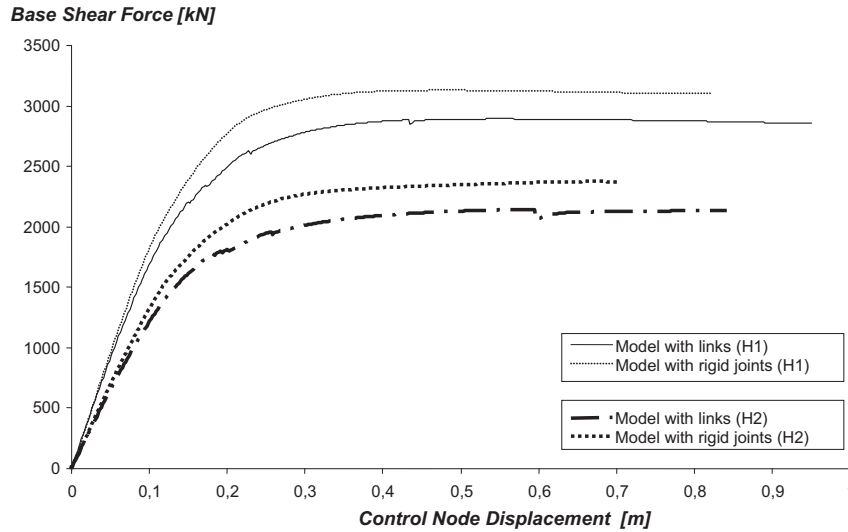
Base Shear Force [kN]

Fig. 13. Capacity Curve of R.C. frame of the Unit N.1 – Horizontal forces proportional to floor mass (H1)–Horizontal forces proportional to first mode (H2).

Table 10
Comparison between pushover analyses carried out by one-dimensional models with rigid joints and with links; F maximum base shear force; K^* initial stiffness of the equivalent non-linear SDF [8,9]; μ ductility in displacement; d_{max} displacement demand.

Type of horizontal forces		Model with rigid joints	Model with links	% Δ
Proportional to floor mass (H1)	F (kN)	3129	2892	8.2
	K^* (kN/m)	18054	16633	8.5
	$\mu = d_u^*/d_y^*$	4.8	5.6	−14.3
	$d_{max} = S_{De}(T^*) \cdot \Gamma$ (m)	0.11	0.12	−6
Proportional to first mode (H2)	F (kN)	2349	2121	10.7
	K^* (kN/m)	13295	12224	8.7
	$\mu = d_u^*/d_y^*$	4.1	4.8	−14.5
	$d_{max} = S_{De}(T^*) \cdot \Gamma$ (m)	0.13	0.14	−7.1

where ε_t is the concrete strain $\varepsilon_t = \frac{\sigma_t}{E_{cls}}$ with σ_t is the cracking concrete stress.

In particular the shear corresponding to joint's collapse V_n is estimated by minimum value between (3) and (4) where N is evaluated considering only vertical loads and the effect of the shear in the column is neglected in first approximation.

The ultimate link bending moment, corresponding to joint collapse, is $M_{yj} = V_n z$ with z the length of the internal lever arm; at this bending corresponds the rotation θ_{yj} (Fig. 12).

The ultimate beam chord rotation capacity can be estimated by [9]:

$$\theta_u = \frac{1}{\gamma_{el}} \left(\theta_y + (\phi_u - \phi_y)L_{pl}\left(1 - \frac{0.5 \cdot L_{pl}}{L_v}\right)\right) \qquad (10)$$

where ϕ_u is the ultimate curvature at the end section.

However the results of the two-dimensional numerical model applied to the considered joints showed that the previous ultimate rotation (relative to the beam) cannot be obtained when the column-beam joint collapses. From the performed analyses and analogous results reported in literature, the ultimate rotation has been assumed to be 30% of (10) [32].

As example, the comparison between the $M–\Theta$ law relative to the beam and to the link, for the fourth floor of the frame (case A), is reported in Fig. 12.

The correctness of the proposed link element was checked by comparison with experimental and numerical analyses. At first the $T5$ specimen was considered; in this case the one-dimensional model results, with and without link, were compared

with those obtained by experimental tests; the collapse type, drift and maximum horizontal force are reported in Table 9. Moreover the joint A of the case study was taken into account, the comparisons among results obtained by one-dimensional model, with and without link, and those obtained by two-dimensional finite element model are reported in Table 9.

In particular the introduction of the link element allows to describe the brittle collapse of joint $(B + J)$ corresponding to the maximum horizontal load T_u that involves the ultimate link bending moment M_{yj}; the ultimate beam chord rotation θ_{uj} permits to obtained an adequate estimation of the ultimate displacement d_u.

8. Pushover analysis by one-dimensional structural model with link elements

Using links in every joints, the pushover analysis of the frame has been repeated. The comparison between the capacity curves are shown in Fig. 13 with horizontal forces proportional to floor mass and proportional to first mode.

The synthesis of the results is reported in Table 10. It should be noted that the numerical model with rigid joints gives an overestimation of the maximum base shear force (on average ≈ 9%) respect to the model with links that instead has a greater ductility (≈14%). In fact the damage of the joints reduces the bending moment in the external columns; this delays the activation of the panel mechanics (the frame with rigid joints collapses by a panel mechanics at the second floor).

Furthermore the stiffness reduction of structure with links entails an increase of the own period of the equivalent non-linear SDF with a increase ($\approx$7%) of the displacement demand $d_{max} = S_{De}(T^*) \cdot \Gamma$ where S_{De} is the elastic displacement response spectrum, T^* is the period of the idealised equivalent SDOF system and Γ is the transformation factor (Table 10).

9. Conclusions

Starting from the seismic vulnerability analysis of the R.C. bearing frame of the Unit N.1 of the Santa Maria Annunziata Hospital in Florence (Italy), the topic relative to the brittle collapse of beam-column joints and its effects on seismic response has been examined. This topic assumes a relevant importance regarding older existing structures that were designed considering only the vertical loads.

In order to take into account the joint damage, a link element, placed between beam and column, has been proposed and introduced in R.C. planar frame one-dimensional numerical model.

The effectiveness of the proposed model is in the using of a simplified approach with a tri-linear moment–rotation law according with European and Italian standard codes. The characteristics of the link can be estimated by limited information, which is a typical situation on older existing structures, and by standard code recommendations. These features can be eventually verified by a two-dimensional finite element model that has been developed in this paper and checked by comparison with experimental tests.

The obtained results highlighted that the analysis with rigid joints can give an unreliable estimation of the capacity curve in terms of maximum base shear and ductility. If a check on other and different cases is necessary, the proposed procedure appears adequate for a pushover analysis in order to give a preliminary evaluation of the seismic capacity for existing R.C. frames.

References

[1] Mitra N. An analytical study of reinforced concrete beam-column joint behavior under seismic loading. Ph.D. Thesis. Department of Civil and Environmental Engineering, University of Washington; 2007.

[2] Fardis MN. A European perspective to performance-based seismic design, assessment and retrofitting. In: Proceedings of international workshop: performance-based seismic design concepts and implementation. Bled, Slovenia, 28 June–1 July 2004.

[3] Pagni CA, Lowes LN. Tools to enable prediction of the economic impact of earthquake damage in older RC beam-column joints. In: Proceedings of international workshop: performance-based seismic design concepts and implementation. Bled, Slovenia, 28 June–1 July 2004.

[4] Paulay T, Priestley MJN. Seismic design of reinforced concrete and Masonry buildings. New York: J. Wiley; 1992.

[5] Birely AC, Lowes LN, Lehman DE. A model for the practical nonlinear analysis of reinforced-concrete frames including joint flexibility. Eng Struct 2012;34:455–65.

[6] Pantazopoulou SJ, Bonacci JF. Consideration of questions about beam-column joints. ACI Struct J 1992;89(1):27–36.

[7] Pampanin S, Calvi GM, Moratti M. Seismic behaviour of R.C. beam-column joints designed for gravity loads. In: 12th European conference on earthquake engineering, London, Paper no. 726; 2002.

[8] NTC 2008, Ministero delle Infrastrutture (2008). DM 14 gennaio 2008, Norme Tecniche per le Costruzioni.

[9] Circolare n. 617 del 2 febbraio 2009. Istruzioni per l'applicazione delle "Nuove norme tecniche per le costruzioni" D.M. 14 gennaio 2008.

[10] El-Metwally S, Chen WF. Moment–rotation modeling of reinforced concrete beam–column connections. ACI Struct J 1988;85(4):384–94.

[11] Alath S, Kunnath SK. Modeling inelastic shear deformation in RC beam-column joints. In: Tenth conference on engineering mechanics. Boulder: University of Colorado; 1995. p. 822–5.

[12] Uma SR, Prasad AM. Analytical modeling of RC beam-column connections under cyclic load. In: Eleventh world conference on earthquake engineering, Acapulco, Mexico.

[13] Kunnath SK. Macromodel-based nonlinear analysis of reinforced concrete structures. Structural engineering worldwide. Paper no. T101-5. Elsevier Science, Ltd., Oxford, England; 1998.

[14] Anderson M, Lehman D, Stanton J. A cyclic shear stress–strain model for joints without transverse reinforcement. Eng Struct 2007;30(4):941–54.

[15] Ghobarah A, Biddah A. Dynamic analysis of reinforced concrete frames including joint shear deformation. Eng Struct 1999;21(11):971–87.

[16] Elmorsi M, Kianoush MR, Tso WK. Modeling bond-slip deformations in reinforced concrete beam-column joints. Can J Civ Eng 2000;27(3):490–505.

[17] Youssef M, Ghobarah A. Strength deterioration due to bond slip and concrete crushing in modeling of reinforced concrete members. ACI Struct J 1999;96(6):956.

[18] Shin M, Lafave JM. Modeling of cyclic joint shear deformation contributions in RC beam–column connections to overall frame behavior. Struct Eng Mech 2004;18(5):645–69.

[19] Tajiri S, Shiohara H, Kusuhara F. A new macroelement of reinforced concrete beam column joint for elasto-plastic plane frame analysis. In: Eighth national conference of earthquake engineering, San Francisco, California.

[20] Lowes LN, Mitra N, Altoontash A. A beam-column joint model for simulating the earthquake response of reinforced concrete frames. Berkeley: Pacific Earthquake Engineering Research Center University of California; 2003.

[21] Altoontash A, Deierlein GD. A versatile model for beam–column joints. In: ASCE structures congress, Seattle, WA.

[22] Lowes LN, Altoontash A. Modeling the response of reinforced concrete beam–column joints. J Struct Eng ASCE 2003;129(12):1686–97.

[23] Mitra N, Lowes LN. Evaluation, calibration, and verification of a reinforced concrete beam–column joint. J Struct Eng 2007;133(1):105.

[24] Jeon J-S et al. Fragility curves for non-ductile reinforced concrete frames that exhibit different component response mechanisms. Eng Struct 2015;85:127–43.

[25] de Witte FC, Kikstram WP. DIANA finite element analysis. User's manual. Analysis procedures. Delft (The Netherlands): TNO DIANA; 2005.

[26] Kupfer HB, Gerstle KH. Behavior of concrete under biaxial stresses. J Eng Mech Div ASCE 1973;99(4):853–66.

[27] Hordijk DA. Local approach to fatigue of concrete. PhD thesis, Department of Civil Engineering, Delft University of Technology, Delft, The Netherlands; 1991.

[28] Cornelissen HAW, Hordijk DA, Reinhardt HW. Experimental determination of crack softening characteristics of normal weight and lightweight concrete. HERON 1986;31(2).

[29] CEB-FIP Model Code 1990, "Desing Code". Comité Euro-Internetional du Béton, Lausanne, Switzerland, Thomas Telford.

[30] Masi A, Santarsiero G, Verderame G, Russo G, Martinelli E, Pauletta M, Cortesia A. Capacity models of beam-column joints: provisions of European and Italian seismic codes and possible improvements. In: Eurocode 8 – Perspectives from the Italian Standpoint Workshop, Napoli, Italy; 2009. p. 145–58

[31] Masi A, Santarsiero G, De Carlo G, Lignola GP, Verderame GM. Test Ciclici su Nodi Esterni Trave-Colonna in C.A.: Confronto tra Risultati Sperimentali e Simulazioni Numeriche. ReLuis-DPC 2005–2008, Napoli; 2009 [in Italian].

[32] Gusella F. Seismic vulnerability assessment of reinforced concrete buildings: modeling of the beam-column joint behaviour and application to S.M.A. Hospital in Bagno a Ripoli, Thesis, Engineering School, University of Florence, Italy; 2013 [in Italian].

[33] SeismoSoft, Inc., SeismoStruct-Computer Program for Static and Dynamic Nonlinear Analysis of Framed Structures, downloadable software with registration from <http://www.seismosoft.com>; 2012.

[34] Mander JB, Priestley MJN, Park R. Theoretical stress–strain model for confined concrete. J Struct Div ASCE 1988;114:1804–26.

[35] Eurocode 8 – Design of structures for earthquake resistance – Part 3: Assessment and retrofitting of buildings, BS EN 1998-3, 2005.